Real-time Observation of Molecularly Thin Lubricant Films on Head Sliders Using Rotating-Compensator-Based Ellipsometric Microscopy

K. Fukuzawa, K. Miyata, C. Yamashita, S. Itoh, H. Zhang

***Abstract*— Lubricant transfer or pick-up from a disk to a head slider is a crucial issue in designing the head-disk interfaces of hard disk drives (HDDs). A method is presented for observing thin-lubricant film on a head slider in real time. That is based on ellipsometric microscopy. The use of rotating-compensator ellipsometry (RCE) results in one order of magnitude higher temporal resolution (0.6 frame/s) and several times higher thickness resolution (0.2 nm) compared to null-ellipsometry-based microscopy, which was recently proposed. RCE-based ellipsometric microscopy will be useful in clarifying the mechanism of lubricant pick up for higher density HDDs.**

***Index Terms*— Head-disk interface, Lubricant transfer, Lubricant pick-up, Ellipsometric microscopy, Imaging ellipsometry, Thin film lubrication, Nanotribology**

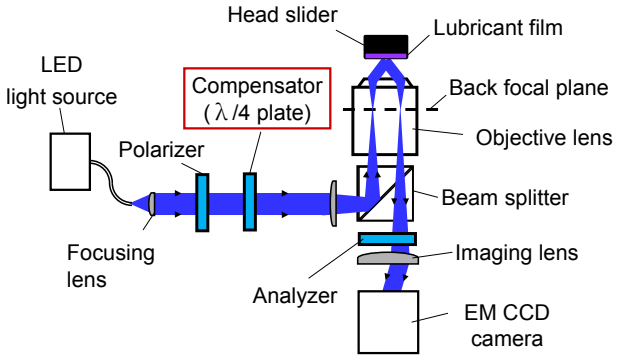

Fig. 1 Schematic of RCE-based VEM.

I. Introduction

Lubricant pick-up by head sliders has become an important issue in head-disk interface (HDI) design due to the decrease in head-disk clearance in hard disk drives (HDDs) [1]. In heat-assisted magnetic recording, it is a particularly crucial issue because disk heating generates more mobile lubricant molecules [2]. The lubricant that is picked up around a read/write element greatly affects read/write performance; however, its behavior has not been clarified sufficiently. This is because observation of lubricant film around a read/write element is difficult with conventional methods such as an ellipsometer or optical surface analyzer because the lateral resolution (on the order of 10 μm) [3]-[5] is insufficient for the head surface around the read/write element. This surface is not flat; it consists of step structures with a lateral size of the order of 10 μm or less.

A new microscopy for the observation of thin films with an improved lateral resolution of the order of 0.1 μm, called vertical-objective-based ellipsometric microscopy (VEM) has been proposed [6]-[8]. It enables real-time observation of nm-thick lubricant films on magnetic disks [7], and the feasibility of visualizing nm-thick lubricant around the read/write element on a slider has been demonstrated [8]. It uses a null-ellipsometry (NE) based method to quantify lubricant thickness. In this NE-based method, it is necessary to find the minimum signal by rotating two polarization devices, a polarizer and an analyzer. This reduces the frame rate to the order of 0.01 frame/s. Higher temporal resolution is required for the observation with higher lateral resolution, because the smaller sized lubricant films diffuse faster. In addition, the signal-to-noise ratio is low, which reduces the thickness resolution. This is because the light intensity is low when finding the minimum signal.

In this paper, we present an improved method that can provide a higher frame rate (~1 frame/s) and a higher signal-to-noise ratio due to the introduction of rotating-compensator ellipsometry (RCE) to quantify the lubricant thickness.

II. Method for Observing Thin Lubricant Film on Slider by RCE-based VEM

A. Setup of VEM

Figure 1 shows the setup for VEM [7], [8]. By detecting the polarization state of the light reflected from the sample using the polarizer, analyzer, and compensator, VEM can measure the thickness distribution in real time. A quarter-wave plate is

Manuscript was received March 9, 2017. This work was supported in part by JSPS KAKENHI Grant Number 26249013 and Storage Research Consortium.

K. Fukuzawa, K. Miyata, C. Yamashita, and S. Itoh are with the Department of Micro/Nano Systems Engineering and H. Zhang is with the Department of Complex Systems Science, Nagoya University, Furo-cho, Chikusa-ku, Nagoya, Aichi 464-8603 Japan (e-mail: fukuzawa@nuem.nagoya-u.ac.jp).

used as the compensator. Setting of the observation system perpendicular to the sample surface overcomes the problem of a narrow field of view with conventional ellipsometric microscopes [9], [10] and provides high lateral resolution (of the order of 0.1 μm). The objective lens that we used had a high numerical aperture (0.95), and the light source was an LED with a wavelength of 460 nm. From the numerical aperture of the objective lens and wavelength of the light source, the lateral resolution was estimated to be 0.3 μm on the basis of the diffraction limit.

B. Measurement of ellipsometric angles of Ψ and Δ

ρ is defined as the ratio of the complex reflectivities for p- and s-polarized lights here, and tanΨ and Δ are defined as the absolute value and argument of ρ, respectively [11].

$$\rho = \frac{r_p}{r_s} = \tan\Psi e^{i\Delta}. \quad (1)$$

The relationship between ellipsometry signal I and compensator angle C generally depends on lubricant thickness h. In RCE methods, h can be quantified by measuring the relationship between I and C when the compensator is rotated.

When the angles of the polarizer and analyzer are set at 0 and 45 degrees with respect to the p-polarization direction, respectively, the relationship between I and C (Fig. 2) is given by [12]

$$I(C) = I_c + I_0(\alpha_4 \cos(4C) + \beta_2 \sin(2C) + \beta_4 \sin(4C)), \quad (2)$$

where

$$\beta_2 = -2\sin 2\Psi \sin\Delta,\ \alpha_4 = -\cos 2\Psi,\ \beta_4 = \sin 2\Psi \cos\Delta. \quad (3)$$

Here, C is defined as the angle between the slow axis of the compensator and the p-polarization direction. In addition, I_c and I_0 are constants determined by the experimental setup. Eq. (2) has a period of 180 deg. The area below the curve is divided into 16 regions at equal intervals as shown in Fig. 2. If T is the period during which the compensator rotates 360 degrees, each interval corresponds to T/16. Letting I_1 to I_{16} be the areas of the divided regions in Fig. 2 and considering Eq. (2) is a periodic function, the coefficients β_2, α_4, and β_4 in Eq. (2) can be obtained through arithmetic processing of I_1 to I_{16} [12].

$$\begin{aligned}
\beta_2 &= I_1 + I_2 + I_3 + I_4 - I_5 - I_6 - I_7 - I_8 + \\
&\quad I_9 + I_{10} + I_{11} + I_{12} - I_{13} - I_{14} - I_{15} - I_{16} \\
\alpha_4 &= I_1 - I_2 - I_3 + I_4 + I_5 - I_6 - I_7 + I_8 + \\
&\quad I_9 - I_{10} - I_{11} + I_{12} + I_{13} - I_{14} - I_{15} + I_{16} \\
\beta_4 &= I_1 + I_2 - I_3 - I_4 + I_5 + I_6 - I_7 - I_8 + \\
&\quad I_9 + I_{10} - I_{11} - I_{12} + I_{13} + I_{14} - I_{15} - I_{16}.
\end{aligned} \quad (4)$$

When a CCD camera is used as a detector, the area I_1 to I_{16} can be easily obtained. The number of electrons induced by the light during the exposure time is summed up at each pixel. If the image is captured synchronously with the compensator rotation and the exposure time is set to T/16, the light intensity is summed up during the exposure time. This means that the light intensity of each pixel in the captured image is the light intensity integrated over T/16, which is proportional to I_1 to I_{16}.

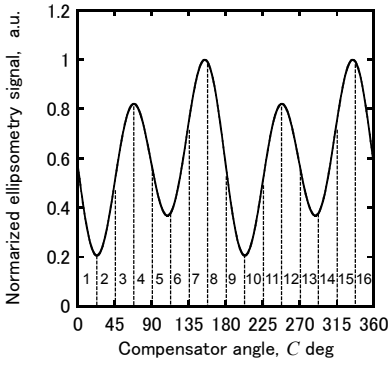

Fig. 2 Relationship between ellipsometry signal and compensator angle.

From Eq. (3), Ψ and Δ can be obtained using β_2, α_4, and β_4.

$$\Psi = \frac{1}{2}\tan^{-1}\left(-\frac{\sqrt{\beta_2^2 + 4\beta_4^2}}{2\alpha_4}\right),\ \Delta = \tan^{-1}\left(-\frac{\beta_2}{2\beta_4}\right). \quad (5)$$

Thus, by measuring the signal intensities for the regions shown in Fig. 2 with a CCD camera, the ellipsometric angles of Ψ and Δ can be obtained for sample surfaces.

In our setup, the ellipsometry signals at all sample points were stored while the compensator was rotated, and the thickness at each point was obtained by analyzing the stored images. This enables to observe lubricant film in real-time. The compensator was rotated using a continuous DC rotary motor stage, whereas a stepping motor stage is needed to find the minimum of the ellipsometry signal in NE-based VEM. In general, the rotation speed of a DC motor is higher than that of a stepping motor. In addition, higher accuracy requires a smaller step increment in NE-based VEM, which reduces the frame rate, whereas accuracy determines the signal-to-noise ratio of the ellipsometry signal in RCE-based VEM. Thus, RCE-based VEM is advantageous in terms of the frame rate. The frame rate is determined by the rotation speed of the compensator in the RCE-VEM. In our setup, one rotation required 1.6 s, which means that a frame rate of 0.6 frame/s is feasible.

C. Measurement of lubricant thickness by RCE-based VEM

In the RCE-based method, the non-lubricated slider surface is first measured by VEM to obtain the ellipsometric angles of Ψ and Δ or the ratio of the complex reflectivities ρ for the non-lubricated surface. Substitution of the measured ρ into Eq. (6) enables the refractive index of the non-lubricated slider surface, N_2, to be obtained:

$$N_2 = N_0 \tan\theta_0 \left[1 - \frac{4\rho}{(1+\rho)^2}\sin^2\theta_0\right]^{\frac{1}{2}}, \quad (6)$$

where N_0 and θ_0 are the refractive index of air and the incident angle. Substitution of N_2 into a three-layer model (air/ lubricant/ head surface) enables the calibration functions of $\Psi(h)$ and $\Delta(h)$ to be numerically obtained for a lubricated slider. The ellipsometric angles of Ψ and Δ or the ratio ρ for the lubricated slider is given by

$$\rho = \tan\Psi(h)e^{i\Delta(h)} = \frac{r_{01p} + r_{12p}\exp(-2id)}{1 + r_{01p}r_{12p}\exp(-2id)} \times \frac{1 + r_{01s}r_{12s}\exp(-2id)}{r_{01s} + r_{12s}\exp(-2id)}, \quad (7)$$

where

$$d = 2\pi N_1 h\cos\theta_1/\lambda,\ r_{ij} = \frac{N_j\cos\theta_i - N_i\cos\theta_j}{N_j\cos\theta_i + N_i\cos\theta_j}. \quad (8)$$

Subscripts 0, 1, and 2 indicate the air, lubricant, and slider surface, respectively, and s and p indicate s- and p-polarized lights, respectively. The calibration functions of $\Psi(h)$ and $\Delta(h)$ were obtained from Eqs. (7) and (8).

After obtaining the calibration functions, we measured a sample slider with lubricant by VEM and obtained measured values of Ψ_m and Δ_m by using a method similar to that for a non-lubricated surface. The thickness of the lubricant on the head surface was obtained so as to minimize the error between the estimated ($\Psi(h_e)$, $\Delta(h_e)$) and the measured (Ψ_m, Δ_m). In this calculation, so as to minimize the errors of both Ψ and Δ, the error E was defined as

$$E \equiv e_\Psi^2 + e_\Delta^2, \quad (9)$$

where

$$e_\Psi = \psi(h_e) - \psi_m,\ e_\Delta = \Delta(h_e) - \Delta_m \quad (10)$$

The update amount of h_e is given by

$$\delta h = -\frac{e_\Psi\frac{\partial e_\Psi}{\partial h} + e_\Delta\frac{\partial e_\Delta}{\partial h}}{\left(\frac{\partial e_\Psi}{\partial h}\right)^2 + \left(\frac{\partial e_\Delta}{\partial h}\right)^2}. \quad (11)$$

The estimation was repeated until δh was below the allowable error.

III. Materials and Experimental Methods

Lubricated head sliders for HDDs were prepared by dip coating. The lubricant was non-polar perfluoropolyether (PFPE) lubricant (Fomblin Z03) with a refractive index of 1.3.

A commercial inverted microscope (IX-71, Olympus Corp.) was modified for the VEM setup (Fig. 1). The objective lens had a high numerical aperture (0.95, MPLANAPO 50X, Olympus Corp.). The light source was an LED (X-Cite, Lumen Dynamics) with a wavelength of 460 nm. To reduce the beam spread angle, a 400-μm-diameter pinhole was placed in front of the light source. The incident angle was 50 deg. The light passed through the polarizer and compensator (quarter-wave plate) before entering the microscope. The compensator was set on a continuous rotation stage (DDR-100, Thorlabs Corp.).

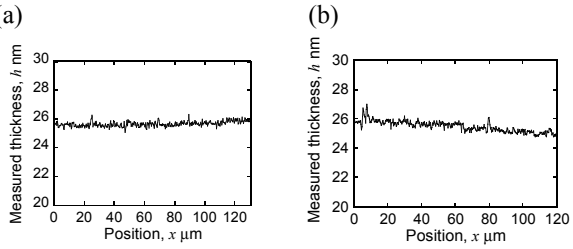

Fig. 3 Thickness distribution of silicon oxide on silicon substrate obtained by RCE-based VEM: (a) x-direction and (b) y-direction distribution on substrate.

The light reflected from the sample passed through the analyzer and was imaged through the imaging lens onto a highly sensitive electron multiplying (EM) CCD camera (Cascade II, Photometrics Corp.). The image was captured synchronously with the compensator rotation. The exposure time was set to be the time obtained by dividing rotation period T by 16, as shown in Fig. 2.

The captured images were stored in a PC. Since the light intensity during the exposure time (T/16) was summed up at each pixel of the CCD camera, the light intensity of the captured image was proportional to the integrated intensity over regions 1 to 16 as shown in Fig. 2. Therefore, by using simple arithmetic image processing (Eq. (4)), followed by calculations using Eq. (5), we can get Ψ and Δ for all sample points at one time, which means the lubricant thickness at all points can be obtained at one time. The image processing for the stored images was done using Image-J software.

IV. Results and Discussion

A. Measurement of standard sample

Figure 3 shows the measured results for a standard sample (a silicon oxide film on a silicon substrate) by the RCE-based VEM. The sample was the calibration sample supplied for the commercial ellipsometer (Five Lab Co., Ltd.). The thickness measured with the ellipsometer was 25.4 nm. Figure 3 shows the thickness distributions in (a) x- and (b) y-directions on the substrate. The values measured by RCE-based VEM agree with the values with the ellipsometer within 0.5 nm. These results support the validity of the RCE-VEM.

B. Measurement of lubricant on head slider

Figure 4 compares the results obtained by NE-based ellipsometric microscope [8] with those by RCE-based one. In the images, the thickness distribution around a read/write element of the slider is shown. The frame rate was 0.6 frame/s for the RCE-based method and 0.02 frame/s for the NE-based one. The frame rate of the RCE-based VEM was one order of magnitude higher than that of the NE-based one. In Fig. 4, the area for one pixel is 0.3 μm x 0.3 μm for the RCE-based VEM and 1.3 μm x 1.3 μm for the NE-based one.

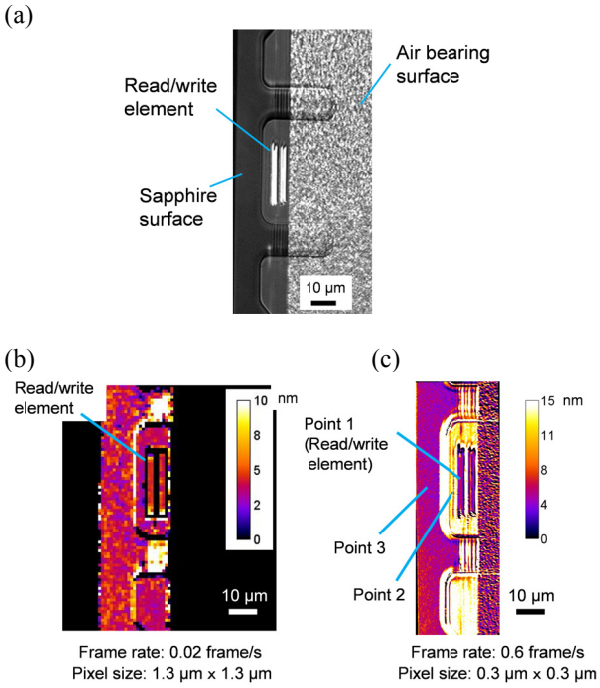

Fig. 4 Comparison between NE- and RCE-based VEM: (a) image of head slider taken by optical microscope, (b) thickness distribution around read/write element measured by NE-VEM, and (c) thickness distribution measured by RCE-VEM.

Figure 5 shows the temporal change in the thickness of the lubricant films from 0 to 16 s at the three sample points shown in Fig. 4(c). Points 1 and 2 are on the surface of the read/write element whereas Point 3 is on the sapphire surface. The mobile lubricant of Point 3 is possible to diffuse to the read/write element surface. The area of each point and the standard deviation of the measured thickness during the 16 s are shown in Table 1. The ellipsometry signal was averaged over the area. The time scale of the lubricant around the read/write element was of the order of 1 min [8]. This means that the thickness did not change significantly during the 16 s. Therefore, the standard deviation in Table 1 can be considered to be measurement noise. In addition, the noise level is proportional to the square root of the measurement or average area, i.e., area of point in Table 1. This enabled us to estimate the thickness resolution at a measurement area of 1 μm x 1 μm by using the results shown in Table 1. A measurement noise of 0.2 nm was obtained for a measurement area of 1 μm x 1 μm as the average value for the three points shown in Table 1. From the reported values for NE-based VEM [8], a thickness resolution of 0.7 nm was obtained for an area of 1 μm x 1 μm. RCE-based VEM thus provided 3.5 times higher resolution than NE-based VEM. This is because the light intensity was higher than that for the NE method. This improvement enabled high-lateral-resolution observation, as shown in Fig. 4.

V. Summary

By using RCE-based ellipsometric microscopy, we attained one order of magnitude higher temporal resolution (0.6 frame/s) and several times higher thickness resolution (0.2 nm) compared to NE-based ellipsometric microscopy. RCE-based ellipsometric microscopy is thus useful for clarifying the mechanism of smaller sized lubricant pick up for higher density HDDs.

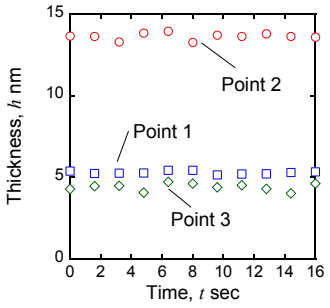

Fig. 5 Temporal change in thickness distribution of lubricant after application for Points 1, 2, and 3 in Fig. 4(c).

Table 1 Measurement error in RCE-VEM

Measurement point	Area of point (μm^2)	Standard deviation (nm)
1	0.3 x 1.3	0.10
2	1.3 x 1.3	0.22
3	1.3 x 1.3	0.22

References

[1] C. M. Mate, B. Marchon, A. N. Murthy, S. -H. Kim, "Lubricant-Induced Spacing Increases at Slider–Disk Interfaces in Disk Drives," *Tribology Letters*, vol. 37, no. 3, pp. 581-590, 2009.

[2] Ji. Rong, T. K. L. Dao, B. X. Xu, J. W. Xu, B. L. Goh, E. Tan, H. Q. Xie, T. Liew, "Lubricant Pickup Under Laser Irradiation," *IEEE Trans. Magn.*, vol. 47, no. 7, pp. 1988–1991, 2011.

[3] V. J. Novotny, I. Hussla, J. - M. Turlet, M. R. Philpott, "Liquid polymer conformation on solid surfaces," *J. Chem. Phys.*, vol. 90, no. 10, pp. 5861-5868, 1989.

[4] S. W. Meeks, W. E. Weresin, H. J. Rosen, " Optical Surface Analysis of the Head-Disk-Interface of Thin Film Disks," *ASME J. Tribology*, vol. 117, pp. 112-118, 1995.

[5] M. F. Toney, C. M. Mate, K. A. Leach, D. Pocker, "Thickness Measurements of Thin Perfluoropolyether Polymer Films on Silicon and Amorphous-Hydrogenated Carbon with X-Ray Reflectivity, ESCA and Optical Ellipsometry," *J. Colloid Interface Sci.*, vol. 225, no. 1, pp. 219-226, 2000.

[6] K. R. Neumaier, G. R. Elender, E. Sackmann, R. Merkel, "Ellipsometric microscopy," *Europhys. Lett.*, vol. 49, no. 1, pp. 14-19, 2000.

[7] K. Fukuzawa, T. Yoshida, S. Itoh, H. Zhang, "Motion Picture Imaging of a Nanometer-thick Liquid Film Dewetting by Ellipsometric Microscopy with a Submicrometer Lateral Resolution," *Langmuir*, vol. 24, no. 20, pp. 11645-11650, 2008.

[8] K. Fukuzawa, C. Yamashita, H. Ishikawa, S. Itoh, H. Zhang, "Measurement of Thickness Distribution of Molecularly Thin Lubricant Films on Head Sliders Using Ellipsometric Microscopy," *IEEE Trans. Magn.*, vol. 52, no. 7, 3300904, 2016.

[9] D. Beaglehole, "Performance of a microscopic imaging ellipsometer," *Rev. Sci. Instrum.*, vol. 59, pp. 2557-2559, 1988.

[10] G. Jin, R. Jansson, H. Arwin, "Imaging ellipsometry revisited: Developments for visualization of thin," *Rev. Sci. Instrum.*, vol. 67, no. 8, pp. 2930-2936, 1996.

[11] R. M. A. Azzam and N. M. Bashara, *Ellipsometry and Polarized Light*, Amsterdam: Elsevier, 1986.

[12] H. Fujiwara, *Spectroscopic Ellipsometry: Principles and Applications*, Wiley, 2007.